© 2018. Published by The Company of Biologists Ltd | Journal of Experimental Biology (2018) 221, jeb168815. doi:10.1242/jeb.168815

RESEARCH ARTICLE

Biomechanical mechanisms underlying exosuit-induced improvements in walking economy after stroke

Jaehyun Bae[1,2], Louis N. Awad[1,2,3], Andrew Long[1,2], Kathleen O'Donnell[1,2], Katy Hendron[3], Kenneth G. Holt[3], Terry D. Ellis[3,*] and Conor J. Walsh[1,2,*]

ABSTRACT

Stroke-induced hemiparetic gait is characteristically asymmetric and metabolically expensive. Weakness and impaired control of the paretic ankle contribute to reduced forward propulsion and ground clearance – walking subtasks critical for safe and efficient locomotion. Targeted gait interventions that improve paretic ankle function after stroke are therefore warranted. We have developed textile-based, soft wearable robots that transmit mechanical power generated by off-board or body-worn actuators to the paretic ankle using Bowden cables (soft exosuits) and have demonstrated the exosuits can overcome deficits in paretic limb forward propulsion and ground clearance, ultimately reducing the metabolic cost of hemiparetic walking. This study elucidates the biomechanical mechanisms underlying exosuit-induced reductions in metabolic power. We evaluated the relationships between exosuit-induced changes in the body center of mass (COM) power generated by each limb, individual joint power and metabolic power. Compared with walking with an exosuit unpowered, exosuit assistance produced more symmetrical COM power generation during the critical period of the step-to-step transition (22.4±6.4% more symmetric). Changes in individual limb COM power were related to changes in paretic (R^2=0.83, P=0.004) and non-paretic (R^2=0.73, P=0.014) ankle power. Interestingly, despite the exosuit providing direct assistance to only the paretic limb, changes in metabolic power were related to changes in non-paretic limb COM power (R^2=0.80, P=0.007), not paretic limb COM power (P>0.05). These findings contribute to a fundamental understanding of how individuals post-stroke interact with an exosuit to reduce the metabolic cost of hemiparetic walking.

KEY WORDS: Exoskeleton, Gait biomechanics, Gait energetics, Post-stroke gait, Robotics, Stroke rehabilitation

INTRODUCTION

Stroke is a leading cause of long-term disability (Mozaffarian et al., 2015), with 80% of survivors after stroke having difficulty with walking (Gresham et al., 1975). Post-stroke hemiparetic walking is characterized by slow, asymmetric and inefficient gait (Olney and Richards, 1996; Patterson et al., 2008, 2010; Perry et al., 1995). A major contributor to post-stroke walking deficits is impaired paretic ankle function, specifically during the push-off and swing phases of the gait cycle. During push-off, impaired paretic ankle plantarflexion (PF) (Chen et al., 2005; Olney et al., 1991; Peterson et al., 2010) reduces the paretic limb's contribution to forward propulsion (Mahon et al., 2015; Takahashi et al., 2015). During swing phase, impaired paretic ankle dorsiflexion (DF) contributes to impaired ground clearance by the paretic limb, increasing the risk of falling (Weerdesteyn et al., 2008). Together, impaired paretic PF and DF contribute to slow walking speed, inter-limb gait asymmetry in spatiotemporal parameters (Lin et al., 2006) and reduced forward propulsion (Farris et al., 2015). Recent studies have shown a relationship between gait asymmetry and an increased metabolic cost of walking in healthy populations (Ellis et al., 2013; Shorter et al., 2017; Soo and Donelan, 2012) and also clinical populations with gait impairments (Awad et al., 2015; Bonnet et al., 2014; Doets et al., 2009; Farris et al., 2015; Feng et al., 2014; Houdijk et al., 2009). Two of these studies, in particular, suggested that increased gait asymmetry in people post-stroke is correlated with the increased metabolic cost of walking (Awad et al., 2015; Farris et al., 2015). There is thus great interest in the development of post-stroke gait interventions that can reduce the metabolic cost of walking by inducing more symmetrical walking (Finley and Bastian, 2017).

Post-stroke ankle impairments often necessitate the use of an ankle foot orthosis (AFO). AFOs are passive assistive devices with a rigid mechanical structure that prevents foot drop during swing. Unfortunately, AFOs have been shown to inhibit normal push-off during walking and reduce gait adaptability (van Swigchem et al., 2014; Vistamehr et al., 2014). An alternative to the passive ankle support provided by an AFO is an active ankle assistive device that enables modulation of the magnitude, timing and direction of assistance (i.e. PF or DF) based on the desired biomechanical response. Active ankle assistive devices include functional electrical stimulation (Kottink et al., 2004; Lynch and Popovic, 2008) and robotic mechanical assistive devices (Díaz et al., 2011; Shorter et al., 2011; Takahashi et al., 2015). Previous studies using such devices have shown improved paretic ankle function and reduced gait impairment (Awad et al., 2016; Forrester et al., 2016).

Our laboratory has developed lightweight, soft wearable robots (exosuits) that interface with the paretic limb of individuals after stroke via garment-like, functional textile anchors (Bae et al., 2015). Exosuits produce gait-restorative joint torques by transmitting mechanical power generated by off-board (Bae et al., 2015; Ding et al., 2014; Quinlivan et al., 2017) or body-worn actuators (Asbeck et al., 2015; Panizzolo et al., 2016) to the paretic ankle through the interaction of the textile anchors with Bowden cables connected to the actuators. In previous work, we demonstrated that a laboratory-based exosuit testbed consisting of an off-board actuator and two textile modules that independently assisted paretic ankle PF and DF during walking (Awad et al., 2017a; Bae et al., 2015) (Fig. 1) could reduce compensatory gait patterns such as hip hiking and

[1]Paulson School of Engineering and Applied Sciences, Harvard University, 60 Oxford Street, Cambridge, MA 02138, USA. [2]Wyss Institute for Biologically Inspired Engineering, Harvard University, 3 Blackfan Circle, Boston, MA 02115, USA. [3]Department of Physical Therapy & Athletic Training, Boston University, 635 Commonwealth Avenue, Boston, MA 02215, USA.

*Authors for correspondence (walsh@seas.harvard.edu; tellis@bu.edu)

J.B., 0000-0002-7300-4518; L.N.A., 0000-0002-0159-8011; T.D.E., 0000-0001-7067-4527; C.J.W., 0000-0002-2744-917X

Received 22 August 2017; Accepted 7 January 2018

Journal of Experimental Biology (2018) 221, jeb168815. doi:10.1242/jeb.168815

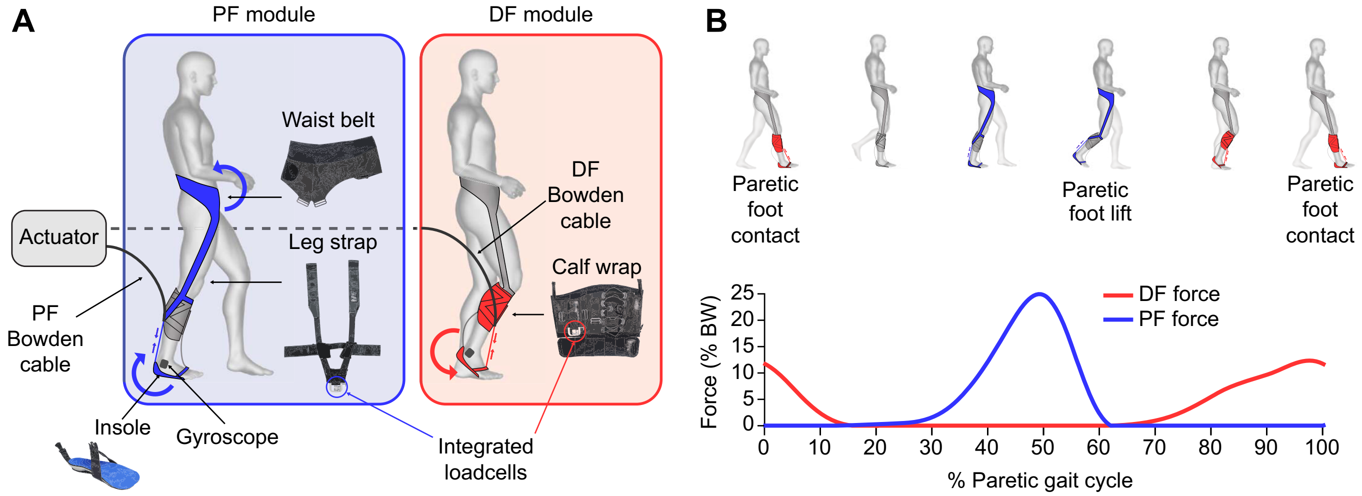

Fig. 1. Exosuit design and operation. (A) A soft exosuit for paretic ankle assistance after stroke. The exosuit consists of two separate textile modules that interface with the paretic limb, a low-profile insole inserted into the paretic shoe, and an off-board actuator that generates the mechanical power transmitted to the wearer's paretic ankle. The first textile module is a plantarflexion (PF) module that anchors at the waist, extends to the paretic leg, and serves as a proximal anchor for a Bowden cable attached posteriorly on the shank. The distal anchor of this Bowden cable is the heel of the low-profile shoe insole. The second textile module is a dorsiflexion (DF) module that anchors around the shank and serves as the proximal anchor for the second Bowden cable, which is attached anteriorly on the shank. The distal anchor for this second Bowden cable is a textile attached to the shoe insole on the dorsal surface of the foot. When retracted by an actuator, Bowden cables transmit mechanical power to the wearer, producing the ankle PF or DF torques. Load cells and gyroscopes are integrated into the exosuit to deliver well-timed assistive force with adequate magnitude through the textiles. (B) Illustration of exosuit actuation (top) and exosuit-generated force trajectory (bottom, where force is given as percentage body weight, % BW), presented with respect to the percentage of the paretic gait cycle. The exosuit delivers to the wearer's ankle PF force during late stance and pre-swing and ankle DF force during swing and initial contact.

circumduction (Awad et al., 2017b), facilitate more symmetric forward propulsive force generation by the paretic and non-paretic limbs, and reduce the metabolic cost of walking (Awad et al., 2017a). Although this previous work demonstrates the substantial impact that exosuits can have on walking after stroke, propulsion symmetry and the metabolic cost of walking are composite variables that can be altered through a variety of biomechanical mechanisms. The objective of this study was thus to identify the specific biomechanical mechanisms underlying exosuit-induced improvements in metabolic power during hemiparetic walking.

Previous studies have demonstrated that the body center of mass (COM) power generated during the step-to-step transition plays a critical role in determining the metabolic cost of walking. Indeed, during this phase of walking when the mass of the body is transferred between limbs, the trailing limb generates COM power to redirect COM velocity while, simultaneously, the leading limb absorbs COM power (Adamczyk and Kuo, 2009; Donelan et al., 2002; Kuo et al., 2005). Simulation and experimental studies have both shown that the COM power generated by the trailing limb during the step-to-step transition is correlated with metabolic power (Donelan et al., 2002; Geyer et al., 2006; Kuo et al., 2005; Soo and Donelan, 2012). When the COM power generated by the individual trailing limbs is asymmetric, metabolic power requirements have been shown to increase in both healthy (Ellis et al., 2013; Soo and Donelan, 2012) and neurologically impaired populations (Bonnet et al., 2014; Doets et al., 2009; Farris et al., 2015; Feng et al., 2014; Houdijk et al., 2009). Individuals with post-stroke hemiparesis generate less COM power from the paretic trailing limb during the step-to-step transition than healthy individuals and compensate for this by generating more COM power from the non-paretic trailing limb (Lamontagne et al., 2007; Peterson et al., 2010; Turns et al., 2007) during the subsequent step-to-step transition. This increased reliance on non-paretic limb COM power generation is correlated with an increased metabolic cost of walking (Stoquart et al., 2012).

Recent work has increased our understanding of the COM power generation during walking. More specifically, through a series of studies, Zelik and colleagues have demonstrated that changes in body COM power result from changes not only in hip, knee and ankle joint power but also in peripheral power (i.e. rate of kinetic power change of the lower limb segments relative to the body COM) and foot power. In 2010, Zelik and Kuo compared individual limb COM power to the sum of the 3 degrees-of-freedom (3DoF) ankle, knee and hip joint rotational power generated during healthy walking (Zelik and Kuo, 2010). Although the limb's positive COM power matched well with the sum of the positive ankle, knee and hip joint power during push-off, during the collision phase of the gait cycle there was a substantial mismatch between the sum of the individual joint powers and the COM power generated. Furthermore, the sum of individual joint powers throughout the gait cycle presented with substantially more positive work than negative work – a paradoxical finding given that positive and negative work should be of equal magnitude during steady-state walking at constant speed. Taken together, these findings demonstrate that the sum of joint powers may not be an accurate reflection of body COM work. Expanding on this work, Zelik et al. (2015) subsequently demonstrated that the relationship between the joint and COM power domains is more complete when accounting for peripheral power, foot power and 3DoF joint translational power (in addition to 3DoF rotational power).

Although COM power may be changed through various biomechanical mechanisms, it has been demonstrated that during the step-to-step transition, the ankle generates the largest power across all the lower extremity joints of the trailing limb in both healthy (Zelik and Adamczyk, 2016) and post-stroke (Farris et al., 2015) populations. Motivated by this biomechanical understanding of COM power generation and its previously defined relationship to metabolic power demands during walking, this investigation focused on evaluating the effects of exosuit assistance of paretic ankle function on the COM power and individual joint power generated by

Journal of Experimental Biology

Journal of Experimental Biology (2018) 221, jeb168815. doi:10.1242/jeb.168815

the paretic and non-paretic trailing limbs. Moreover, we focused our analyses on the double support phase of the gait cycle, which is when the majority of the COM power generated during the step-to-step transition occurs (Adamczyk and Kuo, 2009). A better understanding of how individuals after stroke use the mechanical power provided by exosuits to reduce the metabolic power requirements of walking would advance the field and facilitate the development of more effective wearable assistive devices. We hypothesized that the COM power generated by the paretic and non-paretic trailing limbs during the step-to-step transition would be more symmetric during exosuit-assisted walking than during walking without exosuit assistance and that more symmetric COM power generation would contribute to a reduction in metabolic power. We also hypothesized that more symmetric COM power generation would result from more symmetric ankle power generation.

MATERIALS AND METHODS

Experimental design

An experiment to evaluate the influence of an exosuit designed to improve post-stroke gait mechanics and energetics was conducted on nine individuals in the chronic phase of stroke recovery (Awad et al., 2017a). Participant inclusion criteria included being between the ages of 25 and 75 years; being at least 6 months post-stroke; able to walk for 6 min without stopping or needing the support of another individual; and having sufficient passive ankle range of motion, with the knee extended, to reach a neutral ankle angle. Participant exclusion criteria included receiving Botox within the past 6 months; substantial knee recurvatum during walking; serious comorbidities; inability to communicate and/or be understood by investigators; a resting heart rate outside the range of 50–100 beats min^{-1} or blood pressure outside the range of 90/60 to 200/110 mmHg; pain in the extremities or spine that limit walking; and experiencing more than two falls in the past month. Medical clearance and signed informed consent forms approved by the Harvard University Human Subjects Review Board were obtained from all participants. Two of the nine individuals who participated in this study were excluded from the presented analysis because the way that they walked on the treadmill prevented independent collection of ground reaction forces from the individual limbs, which was required for the study's analyses. Demographics of the remaining seven subjects (age: 49±4 years; time since stroke: 4.38±1.37 years; 44% female; 56% left hemiparetic) are shown in Table 1.

The experiment employed a 2 day testing protocol to evaluate the effects of two different onset timings of exosuit-generated PF force delivery on participants' forward propulsion. Specifically, one of the onset timings was during mid-stance (early onset) and the other timing was during late stance (late onset). The exact timing varied across participants depending on the duration of each participant's paretic stance phase, with the actual commanded PF onset timings averaging 27.5±1.94% of the paretic gait cycle (GC) for early onset and 36.9±0.76% GC for late onset across participants. Our previous study demonstrated that the more effective onset timing varied across participants, and ultimately presented the changes in the metabolic cost of walking from individualized onset timings selected based on the timing that produced the largest improvement in forward propulsion symmetry (Awad et al., 2017a). The present study used the same individualized timings (presented in Table 1).

In each testing session, the participant completed a 5 min standing trial followed by two 8 min walking trials on an instrumented split-belt treadmill. The treadmill speed was set based on participants' overground comfortable walking speeds. The first walking trial consisted of walking with the exosuit completely slack (unpowered) and the second consisted of walking with the exosuit providing active assistance (powered) using one of the onset timings. While walking, participants were allowed, but not encouraged, to hold a handrail. Those who had safety concerns that necessitated holding the handrail in one of the conditions held the handrail in both conditions. None of the participants used an assistive device or orthosis (other than the exosuit) during the walking trials.

Exosuit design and operation

The exosuit used in this study comprises two separate textile modules that securely anchor to the body at the waist and the paretic calf, a low-profile shoe insole that is inserted in a shoe on the paretic foot, and an off-board actuator that generates and transmits mechanical power to the wearer's ankle via Bowden cable retraction (Fig. 1A) (Awad et al., 2017a; Bae et al., 2015). Bowden cables connect the textile modules and an off-board actuator. Mechanical power is generated by the actuator and transmitted to the paretic ankle through retraction of the Bowden cables between the exosuit textiles and insole (Fig. 1B). More specifically, the first textile module, called a PF module, has a multi-articular structure that anchors distally at the paretic calf and proximally at the waist and is designed to generate ankle PF torque. Two straps that extend anteriorly over the thigh and straddle the knee joint center connect the waist and calf anchors of the PF module. Because of its multi-articular structure extending from the anterior hip to the posterior ankle, the PF module generates hip flexion torque concurrently with PF torque (Fig. 1B). The second textile module, called a DF module, anchors at the paretic calf and is designed to generate an ankle DF torque. The overall mass of the exosuit components worn by the wearer is approximately 0.90 kg (waist textile anchor: 0.15–0.20 kg, thigh connecting straps: 0.20–0.22 kg, calf textile anchor and integrated sensors: 0.30–0.35 kg, cables and sheath: 0.12–0.15 kg).

Table 1. Participant characteristics and onset timing of PF actuation

Participant no.	Paretic side	Sex	Age (years)	Chronicity (years)	Mass (kg)	Height (m)	Regular assistive device/orthosis	Treadmill walking speed (m s^{-1})	PF onset timing (% GC)
1	Right	F	30	7.08	49.4	1.62	AFO	1.05*	40.08±1.19
2	Left	M	56	3.58	73.0	1.77	None	1.05	38.15±2.32
3	Left	F	52	0.75	89.7	1.58	Cane	0.53	25.95±0.95
4	Left	M	51	2.83	79.0	1.84	AFO‡ and cane	0.93	33.71±1.09
5	Left	F	37	1.08	79.6	1.72	AFO‡ and cane	0.67	36.82±0.55
6	Right	M	44	2.33	79.7	1.86	None	1.29	35.54±1.55
7	Right	F	46	4.25	60.3	1.67	None	1.3*	33.35±1.57

*Actual 10 m overground walk test speeds were higher than those used on the treadmill. Participant 1's speed was 1.16 m s^{-1}, but this speed was not safe on the treadmill. Participant 7's actual overground speed was 1.72 m s^{-1}, but this speed was beyond the capabilities of the exosuit actuator used for this study.
‡Participant 4 typically used a foot-up brace. Participant 5 used a custom-made brace that supported frontal plane motion.
AFO, ankle foot orthosis; % GC, percentage of gait cycle; PF, plantarflexion.

Journal of Experimental Biology

The off-board actuator contains four linear actuators that allow simultaneous actuation of up to four Bowden cables: only two actuators were used in this study. Each actuator can deliver up to 300 N to the ankle and is equipped with a linear potentiometer (P3 America, Inc., San Diego, CA, USA) that enables closed-loop control of Bowden cable position. Load cells (Futek, Irvine, CA, USA) integrated into the textiles measure the interaction forces between the wearer and exosuit, and shoe-mounted gyroscopes (SparkFun, Niwot, CO, USA) measure foot rotational velocity in the sagittal plane. Together, these sensors enable real-time gait segmentation and iterative force-based position control, and ultimately well-timed assistive forces of adequate magnitude. More specifically, the exosuit controller utilizes measurements from shoe-mounted gyroscopes to detect ground contact events (i.e. initial contact and foot off) for each limb. Exosuit-generated forces are delivered to the wearer based on subphases of the gait cycle determined by these gait events. Our previous work (Bae et al., 2015) showed that the exosuit controller can robustly detect these key events during both the paretic and non-paretic gait cycles and effectively scale the duration of force delivery on a step-by-step basis.

Exosuit-generated force is a composite outcome of the Bowden cable position, the wearer's joint kinematics, and the exosuit–human series stiffness – a parameter that accounts for the mechanical properties of the textiles, Bowden cables and the compliance of the human tissue that supports the textile anchors (Awad et al., 2017a). Because of this, a simple closed-loop position controller with a fixed cable position trajectory is unable to consistently achieve the desired assistive force profiles. To address this challenge, the exosuit controller iteratively adapts the cable position trajectories based on the force measurements from the load cells. The PF controller adapts the Bowden cable position trajectory such that PF force begins to ramp up at a constant onset timing and peaks at a fixed force magnitude during the paretic stance phase. The onset timing and the peak magnitude of the PF force are selected by the research team before testing as a fixed percentage of the paretic gait cycle (% GC) and 25% of subjects' body weight (% BW), respectively (Fig. 1B). In contrast, the DF controller adapts the cable position trajectory to achieve consistent force onset and offset timings and a consistent cable retraction magnitude during swing. The onset and offset timing were selected by the research team such that DF assistance was triggered at the beginning of swing phase and diminished after initial foot contact. Unlike PF cable actuation, a maximum retraction position of the DF cable was selected by the research team before testing and set to bring the paretic ankle to the neutral position – or the smallest ankle PF angle if neutral was not achievable – as identified through visual observation. With this approach, the magnitude of DF force that was delivered to the wearer during the swing phase within and across steps varies with the wearer's gait in a manner that maintains the commanded cable position, and thus ankle angle.

Data collection and analysis

The metabolic cost of walking was assessed by indirect calorimetry by collecting carbon dioxide and oxygen rates using a portable gas analysis system (Cosmed, Rome, Italy). Reflective markers were placed on anatomical bony landmarks and on the Bowden cable anchor connection points for use in gait analysis. Three-dimensional (3D) motion capture was performed at 120 Hz using a Vicon motion capture system (Vicon, Oxford Metrics, Yarnton, UK). An instrumented split-belt treadmill collected 3D ground reaction forces for individual limbs at 960 Hz. Marker positions and ground reaction forces were filtered using a zero-lag low-pass 4th-order Butterworth filter with a cut-off frequency selected from residual analysis (5–9 Hz) (Winter, 2009). Data were also collected from the load cells and gyroscopes integrated into the exosuit at 1 kHz. All data were time synchronized through Matlab and the Vicon Nexus motion capture software. The last 20 strides from each 8 min walking trial with ground reaction forces not contaminated by cross-over steps were used for data analysis.

Metabolic power was calculated using the modified Brockway equation (Brockway, 1987) for the standing and walking trials and was averaged over the last 2 min of walking for each condition. Net metabolic power was obtained by subtracting the average metabolic power measured during the standing trial from the average metabolic power measured during each walking condition. Net metabolic power was normalized by body mass.

The individual limb body COM power was calculated using the individual limb method (Donelan et al., 2002). In brief, this method integrates the sum of the two ground reaction forces divided by the body mass to obtain a body COM velocity with boundary conditions over a given stride such that (1) the average velocity in the anterior–posterior direction is equal to the treadmill speed and (2) there is no net velocity change in other directions. The individual limb COM power is then computed as the integral of the dot product of the COM velocity vector with the individual ground reaction force vector. Joint kinematics were calculated using the inverse kinematics method (Visual3D, C-Motion, Rockville, MD, USA). 3DoF joint rotational power (called joint power from here for simplicity) were calculated using the inverse dynamics method based on joint kinematics and ground reaction force data.

The markers located on the Bowden cable attachment points on the textiles and the insole were used to calculate the moment arms of the Bowden cable with respect to the ankle joint. The exosuit-generated ankle moment was calculated by multiplying the moment arm and the measured Bowden cable force. The exosuit-generated joint power was then calculated by multiplying the exosuit-generated joint moment and the joint velocity calculated through inverse kinematics.

Normalization and statistical analysis

Metabolic and biomechanical power variables were normalized to body mass to produce units of W kg^{-1} for statistical comparison. Individual limb/joint power data from each stride were then divided into four different phases: paretic limb single support, paretic limb double support (defined as non-paretic heel strike to paretic toe-off), non-paretic limb single support, and non-paretic limb double support (defined as paretic heel strike to non-paretic toe-off). The primary biomechanical variables analyzed were positive individual limb COM power and ankle, knee and hip joint power averaged during each limb's respective trailing limb double support (TDS). This was based on an understanding that the trailing limb generates the majority of body COM power for the step-to-step transition during double support (Adamczyk and Kuo, 2009; Donelan et al., 2002).

A symmetry index (SI) was used to evaluate inter-limb asymmetry of the biomechanical variables. The symmetry index was defined as:

$$\mathrm{SI} = \left|\frac{X_{\mathrm{np}} - X_{\mathrm{p}}}{0.5\ (X_{\mathrm{np}} + X_{\mathrm{p}})}\right| \cdot 100\,(\%), \tag{1}$$

where X_{np} and X_{p} are, respectively, the biomechanical variables from the non-paretic and paretic limb (Nadeau, 2014). This index is always positive or zero, and 0% means perfect symmetry. Statistical analysis was conducted in Matlab (MathWorks, Natick, MA, USA). One-sample paired *t*-tests compared the two conditions (exosuit unpowered and powered) to evaluate the effects of exosuit assistance. For variables studied across the gait cycle, statistically significant differences were confirmed only with consecutive rejection of the null hypothesis for more than 4% of the gait cycle. Linear regression was performed to investigate the correlation between the different biomechanical variables, and an F-test was performed on the regression model to assess the strength of the correlation. The statistical significance level was set at P<0.05 for all analyses.

RESULTS

Individual limb COM power across the gait cycle and during trailing limb double support

During walking with the exosuit unpowered, participants' non-paretic limbs generated 0.46±0.06 W kg^{-1} of positive COM power and −0.29±0.04 W kg^{-1} of negative COM power across the gait cycle (Fig. 2A, right). In contrast, their paretic limbs generated 0.18±0.04 W kg^{-1} of positive COM power and −0.29±0.04 W kg^{-1} of negative COM power (Fig. 2A, left). With the exosuit powered, participants reduced the positive COM power generated from their non-paretic limbs by 11.3±4.2% to 0.40±0.05 W kg^{-1} (P=0.0407) and reduced the negative COM power generated from their paretic limbs by 9.0±3.7% to −0.26±0.05 W kg^{-1} (P= 0.0174). It should be noted that the average paretic limb's positive COM power increased to 0.20±0.04 W kg^{-1}, but this change did not reach our *a priori* threshold for significance (P=0.0521).

Focusing the analysis on the positive power generated by the paretic and non-paretic trailing limbs during double support (gray shading in Fig. 2A, Table 2), we observed that participants generated 0.21±0.04 W kg^{-1} of positive COM power from their non-paretic limbs and 0.12±0.02 W kg^{-1} from their paretic limbs (i.e. 56.48±15.21% SI; Fig. 2B) during walking with the exosuit unpowered. With the exosuit powered, participants increased the positive COM power generated from their paretic limbs by 22.9±9.42% to 0.14±0.02 W kg^{-1} (P=0.016), contributing to 39.06±7.78% more symmetric positive COM power generation between limbs during trailing limb double support (i.e. new SI of 34.07±10.27%, P=0.0112) (Fig. 2B).

Correlation between individual limb COM power during trailing limb double support and net metabolic power

Linear correlations were observed between net metabolic power – computed as metabolic power during walking less the metabolic power at rest – and the positive COM power generated during trailing limb double support by the non-paretic limb, but not the paretic limb, in both the exosuit unpowered (R^2=0.77, P=0.009) and powered (R^2=0.58, P=0.047) conditions (Fig. 3A). Similarly, a reduction in non-paretic limb positive COM power during trailing limb double support was associated (R^2=0.80, P=0.007) with a 10.43±1.48% reduction in net metabolic power that was observed between testing conditions (suit unpowered: 4.18±0.43 W kg^{-1}, powered: 3.72±0.34 W kg^{-1}, P=0.005) (Fig. 3B).

Lower-limb joint power generated during trailing limb double support

A deeper investigation into the exosuit's effects on power generation during trailing limb double support was subsequently conducted by summing the joint power generated across the individual joints of the lower extremities, with and without the exosuit powered (Fig. 4 and Table 2). When walking with the exosuit unpowered, the non-paretic lower limb joints (i.e. ankle, knee and hip) as a whole generated

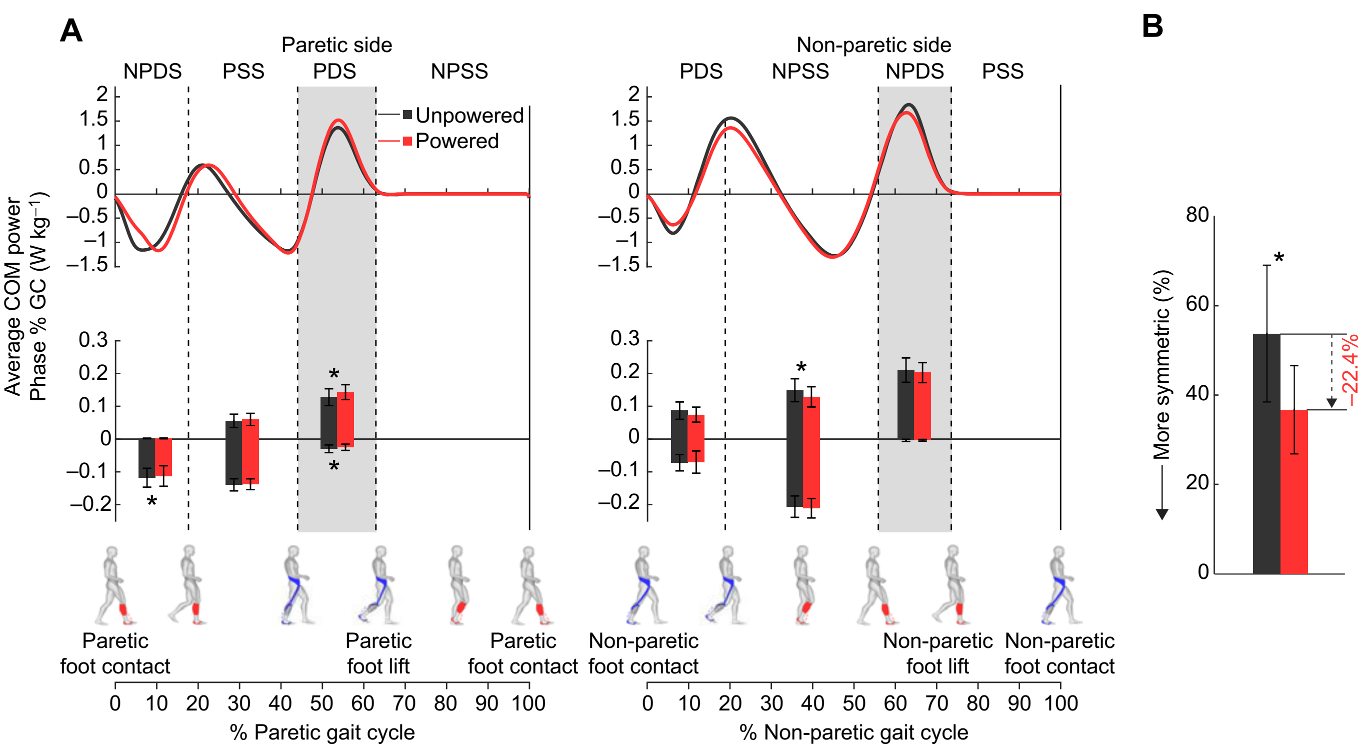

Fig. 2. Individual limb COM power across the gait cycle. (A) Group average center of mass (COM) power segmented into percentage gait cycle (top) and sub-phases (bottom) for two different conditions (exosuit unpowered and powered) on the paretic and non-paretic limbs. The gait cycle was divided into four different sub-phases representing paretic and non-paretic limb double support (PDS and NPDS) and single support (PSS and NPSS). Trailing limb double support for each limb is indicated with gray shading. (B) Symmetry indices of average positive COM power generation during the trailing limb double support. These indices represent interlimb symmetry of positive COM power generated during the trailing limb double support (gray shading in A). *Statistically significant change from exosuit unpowered to powered condition.

Table 2. Positive power generated during trailing limb double support and their inter-limb symmetry

	Non-paretic power (W kg^{-1})		Paretic power (W kg^{-1})		Inter-limb symmetry (%)	
	Unpowered	Powered	Unpowered	Powered	Unpowered	Powered
Body COM	0.213±0.039	0.201±0.033	**0.123±0.024**	**0.143±0.023***	**56.487±15.212**	**34.069±10.272***
Sum of joints	0.247±0.034	0.230±0.036	0.132±0.035	0.130±0.032	72.041±18.534	60.310±15.277
Ankle	0.227±0.038	0.210±0.039	0.115±0.032	0.116±0.030	**70.871±19.087**	**60.665±19.057***
Knee	0.020±0.008	0.022±0.009	0.035±0.012	0.039±0.015	116.658±25.364	118.865±21.667
Hip	0.094±0.009	0.093±0.010	0.069±0.009	0.054±0.011	**43.346±9.621**	**58.781±11.604***

COM, center of mass.
*Statistically significant changes from exosuit unpowered to powered condition (P<0.05).

0.25±0.03 W kg^{-1} of positive power with minimal negative power absorption (−0.005±0.003 W kg^{-1}). The paretic lower limb joints generated 0.13±0.03 W kg^{-1} of positive power, significantly less than the non-paretic limb joints (P=0.0198, SI=72.04±18.53%), and absorbed a non-negligible amount of negative power (−0.04±0.01 W kg^{-1}) (Fig. 4A). When powered, the exosuit delivered 0.017±0.003 W kg^{-1} of positive power to the paretic ankle with minimal negative power absorption (−0.0032±0.0015 W kg^{-1}) (Fig. 4B). Because of the multi-articular structure of the PF module, the exosuit concurrently delivered 0.0099±0.0024 W kg^{-1} of positive power and absorbed −0.0052±0.0017 W kg^{-1} of negative power at the paretic hip. Despite the observed changes in individual limb COM power (described above), changes in the positive joint power generated across the lower limb joints were not observed in either the paretic or non-paretic limbs, or in their symmetry (Ps>0.05; see Table 2).

Focusing our analysis on individual joint power generation during the trailing limb double support, we observed that positive ankle power generation was significantly asymmetric when walking with the exosuit unpowered; the non-paretic ankle generated significantly more positive power than the paretic ankle (non-paretic ankle: 0.23±0.04 W kg^{-1}, paretic ankle: 0.11±0.03 W kg^{-1}, SI=70.87±19.08%). With the exosuit powered, positive ankle power asymmetry reduced to 60.66±19.05% (P=0.049); however, changes in individual joint positive ankle power generation were not observed (Table 2). Individuals' hip joints produced substantially lower positive power during the trailing limb double support than the ankle joints when walking with the exosuit unpowered (non-paretic hip: 0.094±0.009 W kg^{-1}, paretic hip: 0.069±0.009 W kg^{-1}), but were also asymmetric (SI=43.346±9.621%). Unlike the ankle joint power, hip joint power generation became more asymmetric with the exosuit powered (SI=58.781±11.604%, P=0.0256), despite the absence of statistically significant changes in either the paretic or non-paretic hip joints (Ps>0.05). The paretic and non-paretic knee joints generated relatively low positive power during the trailing limb double support, and changes in knee power with the exosuit powered were not observed (P>0.05, see Table 2).

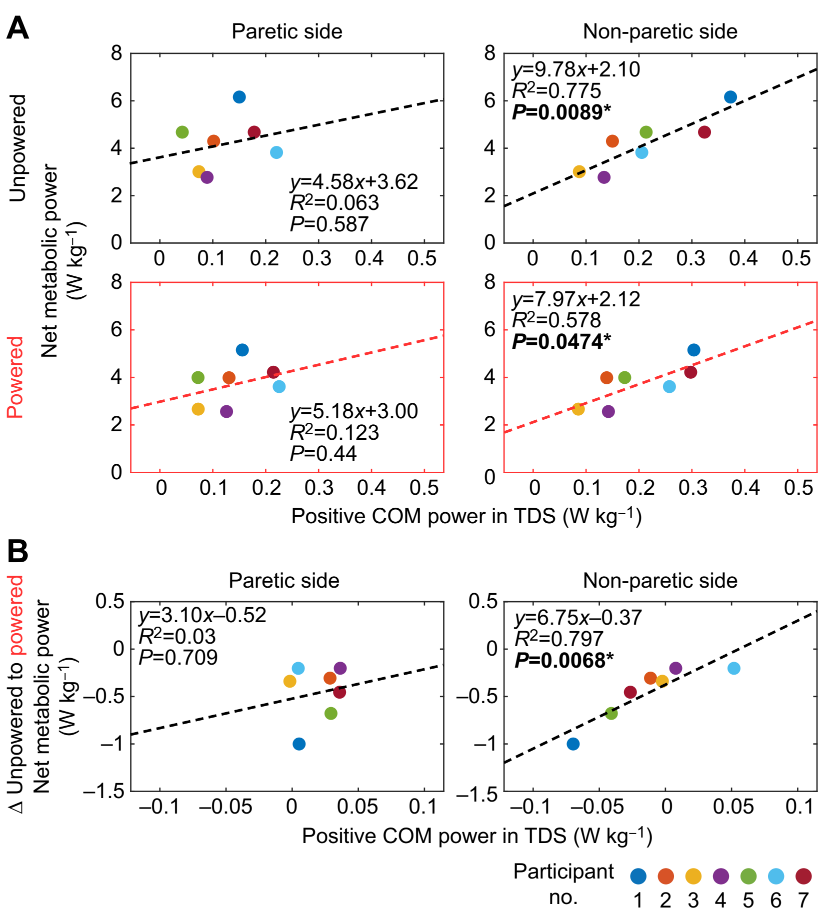

Fig. 3. Correlation between COM power during trailing limb double support and net metabolic power. (A) Correlation of average positive COM power generated in trailing limb double support (TDS; x-axis) and average net metabolic power (y-axis) for the exosuit unpowered (top) and exosuit powered (bottom) conditions. Non-paretic COM power was linearly correlated to net metabolic power (P<0.05) in both conditions, while the correlation between paretic COM power and metabolic power was not statistically significant in either condition. (B) Correlation of the change in average positive COM power during trailing limb double support and the change in net metabolic power resulting from exosuit assistance. Exosuit-induced net metabolic power reduction was linearly correlated with the exosuit-induced change of non-paretic positive COM power during trailing limb double support, whereas a statistically significant correlation with paretic positive COM power was not observed. TDS, trailing limb double support.

Journal of Experimental Biology (2018) 221, jeb168815. doi:10.1242/jeb.168815

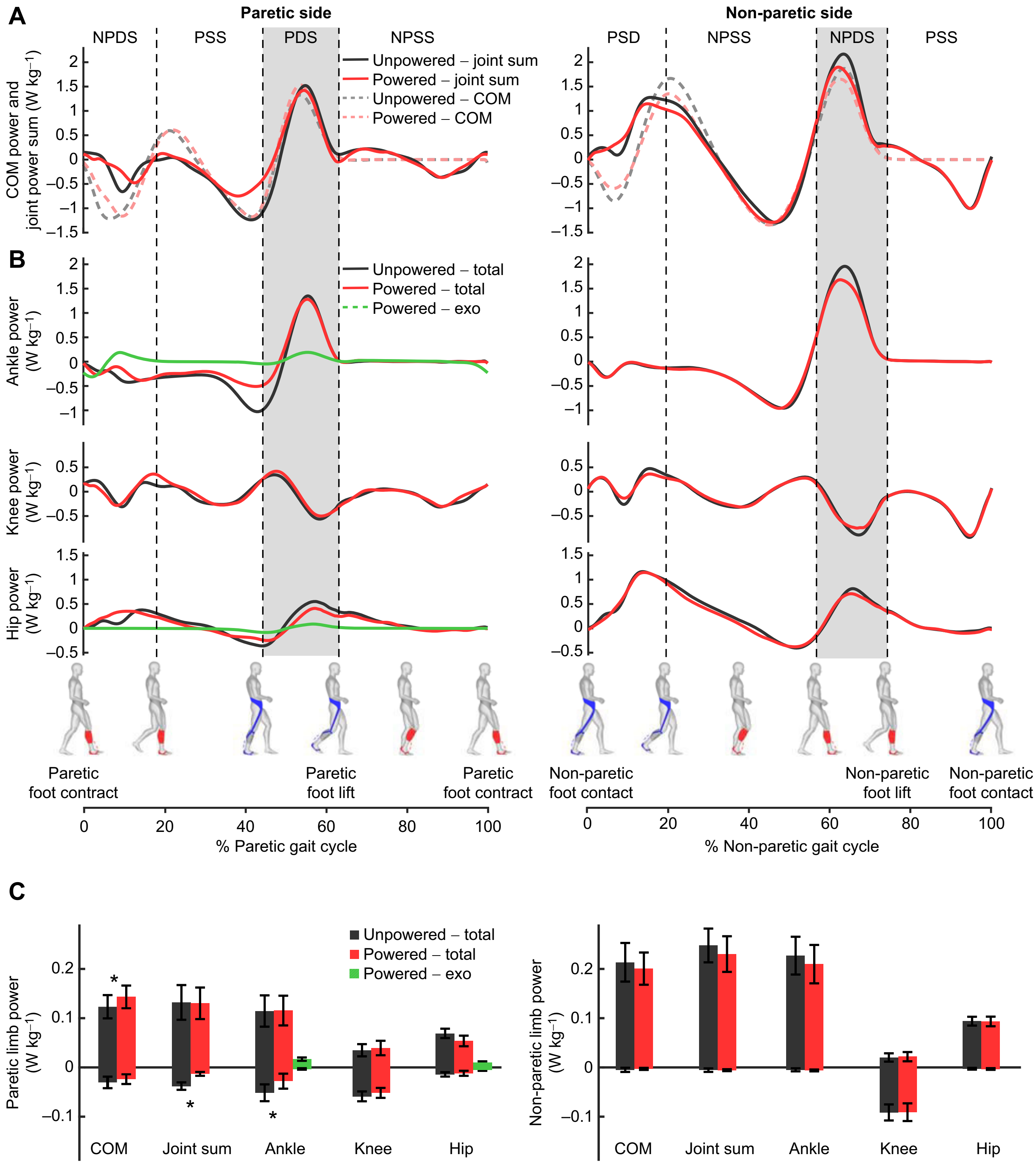

Fig. 4. Individual joint power across the gait cycle. (A) Group average of body COM power and sum of lower-limb joint power segmented into percentage gait cycle. (B) Group average of ankle, knee and hip joint power segmented into percentage gait cycle. The trailing limb double support phase of each limb is indicated with gray shading. total: total power generated by human and exosuit; exo: ankle and hip power generated by exosuit when powered. (C) Average of positive and negative power variables generated during the trailing limb double support (gray shading in A,B). *Statistically significant difference between the exosuit powered and unpowered conditions. Note that ankle and hip power generated by the exosuit is zero in the unpowered condition.

Journal of Experimental Biology (2018) 221, jeb168815. doi:10.1242/jeb.168815

Relationship between ankle power and total limb COM power during trailing limb double support

Given the concurrently observed exosuit-induced changes in the interlimb symmetry of the ankle and COM positive power generated during the trailing limb double support (Table 2), the correlation between these variables was evaluated. Linear correlations were observed between the positive ankle power and positive COM power generated during trailing limb double support for both the paretic and non-paretic limbs during both the exosuit unpowered and powered conditions (R^2>0.77, P<0.009) (Fig. 5A). Similarly, for both conditions, the change in COM power generated by each limb during trailing limb double support correlated with the change in ankle power generated by each limb (R^2>0.73, P<0.014) (Fig. 5B).

Relationship between ankle joint power during trailing limb double support and net metabolic power

Similar to the relationship between metabolic power and the positive COM power generated by the individual limbs during trailing limb double support (Fig. 3A), we observed linear correlations between metabolic power and non-paretic (but not paretic) ankle positive power during both the exosuit unpowered (R^2=0.77, P=0.009) and powered (R^2=0.65, P=0.028) conditions (Fig. 6A). However, interestingly, changes in neither non-paretic (R^2=0.44, P=0.105) nor paretic (R^2=0.01, P=0.834) ankle power were correlated with changes in metabolic power (Fig. 6B).

DISCUSSION

This paper presents a systematic investigation into the biomechanical mechanisms underlying the reduced metabolic cost of walking observed during exosuit-assisted walking after stroke. Specifically, we evaluated the effects of walking with an exosuit assisting the paretic ankle on individual limb COM power and joint power, and investigated the relationship between changes in these biomechanical variables and changes in metabolic power. As hypothesized, exosuit assistance contributed to more symmetric COM power generation by each limb during the step-to-step transition and a reduction in metabolic power. Interestingly, it was a reduction in the body COM power generated by the non-paretic limb during the step-to-step transition that strongly correlated with the reduction in metabolic power, with changes in non-paretic ankle power generation strongly contributing to this reduction. Collectively, these findings demonstrate that soft robotic exosuits can assist the paretic ankle during walking in a manner that positively influences whole-body gait mechanics and energetics.

Consistent with previous studies showing that post-stroke walking is energetically inefficient and mechanically asymmetric (Bonnet et al., 2014; Doets et al., 2009; Feng et al., 2014; Mahon et al., 2015), our participants expended 45% more metabolic power than healthy individuals to walk (Collins et al., 2015) and generated substantially less COM power from the paretic limb compared with the non-paretic limb during walking with the unpowered exosuit (Fig. 2). Our observation that the COM power generated by the non-paretic limb during trailing limb double support was positively correlated with metabolic power during walking with an unpowered exosuit (Fig. 3A) also concurs with previous work (Stoquart et al., 2012). Building on this previous understanding of post-stroke gait mechanics and energetics, our findings demonstrate that exosuit-induced reductions in non-paretic limb COM power generation

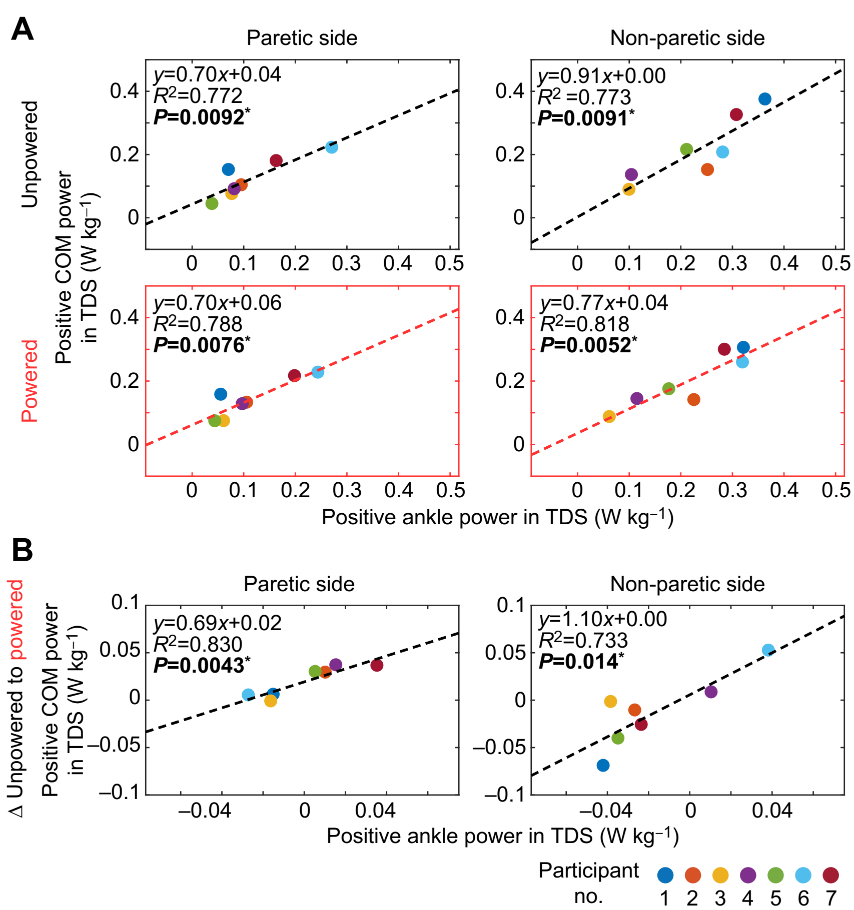

Fig. 5. Correlation between ankle and COM power during trailing limb double support. (A) Correlation of average positive ankle power (*x*-axis) produced during trailing limb double support and average positive COM power over the same time period (*y*-axis) for the exosuit unpowered and powered condition. Positive ankle power was linearly correlated with positive COM power on both limbs in both conditions (P<0.05). (B) Correlation of the change of average positive ankle power and the change of COM power in exosuit-assisted walking. Exosuit-induced ankle power change was linearly correlated to the exosuit-induced change of positive COM power during trailing limb double support on both limbs (P<0.05). TDS, trailing limb double support.

Journal of Experimental Biology (2018) 221, jeb168815. doi:10.1242/jeb.168815

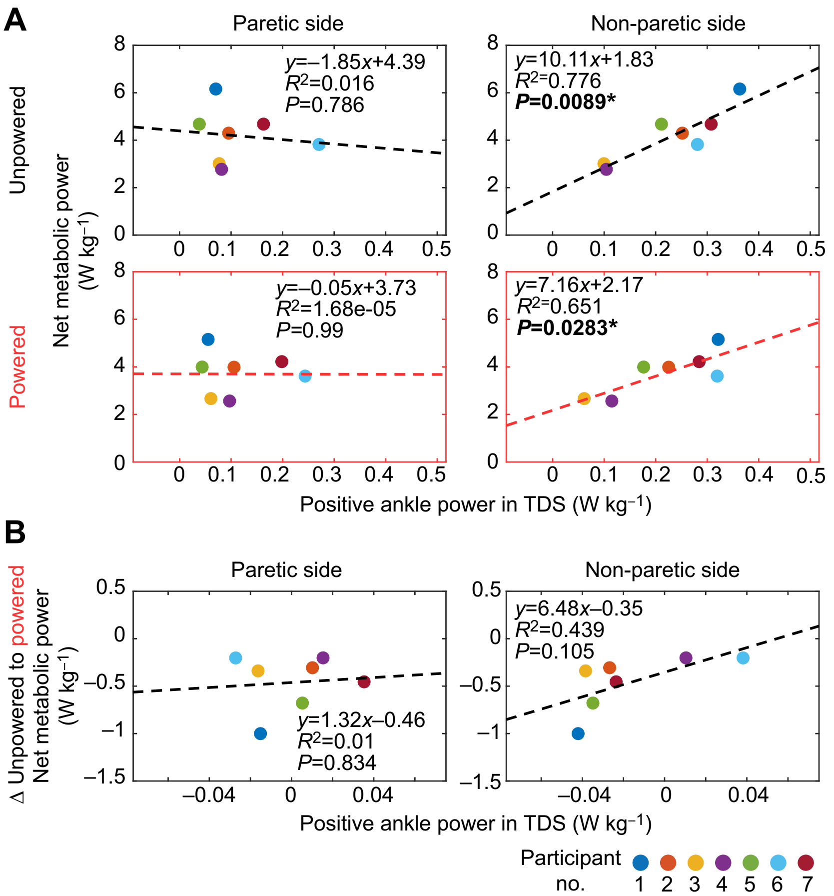

Fig. 6. Correlation between ankle power during trailing limb double support and net metabolic power. (A) Correlation of average positive ankle power (*x*-axis) generated during trailing limb double support and net metabolic power (*y*-axis) for the exosuit unpowered and powered conditions. Non-paretic ankle power was linearly correlated to net metabolic power (P<0.05) in both conditions. The correlation between paretic ankle power and metabolic power was not statistically significant for either condition. (B) Correlation of the changes in average positive ankle power and net metabolic power in exosuit-assisted walking. No statistically significant correlation was found between exosuit-induced ankle power changes and changes in metabolic power (P>0.1). TDS, trailing limb double support.

during the step-to-step transition contribute to reductions in metabolic power (Fig. 3B). This was surprising given that exosuits provide direct assistance to only the paretic limb. These findings suggest that individuals after a stroke are able to leverage the mechanical assistance provided to the paretic ankle to reduce a reliance on the non-paretic limb for walking. Indeed, other work has shown that individuals after stroke have a compensatory reliance on the non-paretic limb that can be altered with gait retraining (Hsiao et al., 2016). Our finding that exosuits produced a similar change in inter-limb dynamics without any gait training provides compelling evidence for the promising use of exosuits to deliver targeted gait assistance during hemiparetic walking.

It is interesting to note that despite observing changes in the positive COM power produced by the paretic limbs when walking with the powered exosuit, we did not observe changes in the sum of the positive power produced by the hip, knee and ankle joints. This finding may be explained by prior work by Zelik and colleagues that demonstrated the importance of accounting for peripheral power, foot power and 3DoF joint translation power in addition to the traditionally evaluated 3DoF joint rotational power (Zelik and Kuo, 2010; Zelik et al., 2015). Although validation of this hypothesis is beyond the scope of this study, in our prior work, we observed exosuit-induced reductions in limb circumduction and hip hiking (Awad et al., 2017b). Such changes in foot and pelvis trajectories relative to the COM suggest a substantial reduction in peripheral power. A reduction in peripheral power without concurrent changes in joint power may explain the observed mismatch between changes in COM and joint power. Moreover, our previous report of the effects of exosuit-assisted walking on the anterior ground reaction force generated by the limb during walking (Awad et al., 2017a) suggests changes in foot power (Takahashi et al., 2012). Further study is required to reveal the exact source of COM power changes during exosuit-assisted walking.

Our findings that positive ankle joint power and COM power during trailing limb double support concurrently became more symmetric when walking with the exosuit powered (Table 2), and that exosuit-induced changes in these variables were highly correlated (Fig. 5), suggest that targeted assistance of the paretic ankle is an effective strategy to improve gait mechanics after stroke at both the individual joint and whole-body levels. Future research into how targeted assistance of the biomechanical deficits of the paretic limb influences non-paretic limb biomechanics and overall walking ability after stroke would advance the field of wearable assistive robotics.

Our evaluation of the relationship between the ankle power generated during trailing limb double support and metabolic power (Fig. 6) revealed that the positive power generated by the paretic and non-paretic ankles during their respective step-to-step transitions highly correlated with net metabolic power. It was surprising, however, that exosuit-induced changes in these variables were not related, especially given that changes in ankle power contributed strongly to changes in the body COM power generated by each limb (Fig. 5B), which, as previously discussed, did contribute to changes in metabolic power (Fig. 3B). This finding highlights the complex relationship between the mechanics and energetics of walking after stroke and suggests that, in response to the exosuit's targeted assistance of paretic ankle deficits, users with hemiparesis achieve a metabolic benefit through heterogeneous biomechanical responses (see Figs S1 and S2 for other biomechanical changes) in combination with ankle power generation strategies. Indeed, our

Journal of Experimental Biology (2018) 221, jeb168815. doi:10.1242/jeb.168815

team has recently shown exosuit-induced reductions in whole-limb compensatory gait motions that are known to increase metabolic power (Shorter et al., 2017), such as circumduction and hip hiking (Awad et al., 2017b). Further study into the potential mediating role that exosuit-induced reductions in compensatory walking strategies plays in the relationship between changes in ankle power and metabolic power would enhance our understanding of how active assistance delivered through a wearable robot can improve walking after stroke.

Although this study presents a comprehensive analysis of exosuit-induced changes in post-stroke gait mechanics and energetics, it is limited by a small sample size. However, comparable sample sizes have been used successfully to evaluate other wearable assistive devices (Collins et al., 2015; Malcolm et al., 2013; Mooney et al., 2014; Takahashi et al., 2015) and we believe that the findings of this study provide a meaningful step toward understanding how individuals after stroke utilize robotic ankle assistance to achieve a more economical gait. Another limitation is that this investigation focused on the effects of walking with an exosuit worn unpowered versus powered. Although the exosuit is compliant and lightweight with its mass (~0.9 kg) distributed along the length of the paretic limb, to evaluate the net effect of exosuit assistance on participants' walking behavior, it is important to know whether there are effects due to simply wearing the unpowered exosuit. In a previous study (Awad et al., 2017a), we found that wearing the unpowered exosuit did not influence participants' ability to generate propulsion or their energy cost of walking compared with not wearing the exosuit. This result is consistent with a prior investigation of the effects on hemiparetic walking of additional load worn unilaterally above the paretic ankle (Duclos et al., 2014). These previous studies suggest that an exosuit worn unpowered does not substantially alter the biomechanics of post-stroke walking. Finally, this study used the trailing limb double support phase as a surrogate for the step-to-step transition. The step-to-step transition is often defined based on the change in sagittal plane COM velocity (Adamczyk and Kuo, 2009); however, substantial variability in these data prohibited identification of the step-to-step transition using this approach. The trailing limb double support phase has been widely used to represent the step-to-step transition, and the COM power generated during this phase of the gait cycle has successfully captured the broad trends in positive COM power observed during the step-to-step transition (Adamczyk and Kuo, 2009; Mahon et al., 2015).

In conclusion, this paper demonstrates that a soft robotic exosuit can target deficits in paretic ankle function in a manner that induces more-symmetrical COM power generation and reduced metabolic effort during walking. These findings contribute to a fundamental understanding of how individuals after stroke interact with exosuit-generated paretic ankle assistive forces to reduce the metabolic cost of walking and support the use of exosuits for post-stroke gait assistance and rehabilitation. This work provides insight to guide future research and development of ankle-centered, active, gait assistive devices and their control strategies for individuals with neurologically based gait impairment.

Acknowledgements
We thank Stephen Allen, Fabricio Saucedo and Christopher Siviy for their assistance with data collection and processing. We thank Gabriel Greeley, Tiffany Wong, Ye Ding, Maria Athanassiu, Nicolas Menard, Mike Rouleau, Dr Nikolaos Karavas, Dr Ignacio Galiana and Dr Alan Asbeck for their assistance developing the exosuit. We thank Sarah Sullivan, Madeline Jackson, Naomi Zingman-Daniels, Lauren Bizarro and Dionna Roberts of the Wyss Institute Clinical Research Team for assistance with the study. We thank our study participants who generously gave their time for this research.

Competing interests
Patents have been filed with the U.S. Patent Office describing the exosuit components documented in this paper. J.B., K.G.H., K.O. and C.J.W. were authors of those patents and patent applications (PCT/US2013/60225 – Soft Exosuit For Assistance With Human Motion; PCT/US2014/68462 – Assistive Flexible Suits, Flexible Suit Systems, and Methods for Making and Control Thereof to Assist Human Mobility; PCT/US2014/40340 – Soft Exosuit for Assistance with Human Motion; PCT/US2015/51107 – Soft Exosuit for Assistance with Human Motion). Harvard University has entered into a licensing and collaboration agreement with ReWalk Robotics. C.J.W. and K.O. are paid consultants to ReWalk Robotics.

Author contributions
Conceptualization: J.B., L.N.A., K.G.H., T.E., C.J.W.; Methodology: J.B., L.N.A., A.L., K.O., K.H., K.G.H., T.E., C.J.W.; Software: J.B.; Validation: J.B., L.N.A., A.L., C.J.W.; Formal analysis: J.B., A.L.; Investigation: J.B., L.N.A., K.O., K.H.; Resources: T.E., C.J.W.; Data curation: J.B., A.L.; Writing - original draft: J.B., L.N.A., A.L.; Writing - review & editing: J.B., L.N.A., A.L., K.O., K.H., K.G.H., T.E., C.J.W.; Visualization: J.B.; Supervision: L.N.A., K.O., K.G.H., T.E., C.J.W.; Project administration: K.O., T.E., C.J.W.; Funding acquisition: L.N.A., T.E., C.J.W.

Funding
This work was supported by the Defense Advanced Research Projects Agency (DARPA), Warrior Web Program (contract number W911NF-14-C-0051). The views and conclusions contained in this document are those of the authors and should not be interpreted as representing the official policies, either expressly or implied, of DARPA or the U.S. Government. This work was also partially funded by the National Science Foundation (CNS-1446464), American Heart Association (15POST25090068), National Center for Advancing Translational Sciences of the National Institutes of Health (1KL2TR001411), Rolex Award for Enterprise, Harvard University Star Family Challenge, Wyss Institute for Biologically Inspired Engineering, and Harvard John A. Paulson School of Engineering and Applied Sciences. Deposited in PMC for release after 12 months.

Supplementary information
Supplementary information available online at
http://jeb.biologists.org/lookup/doi/10.1242/jeb.168815.supplemental

References
Adamczyk, P. G. and Kuo, A. D. (2009). Redirection of center-of-mass velocity during the step-to-step transition of human walking. *J. Exp. Biol.* **212**, 2668-2678.

Asbeck, A. T., Schmidt, K., Galiana, I. and Walsh, C. J. (2015). Multi-joint Soft Exosuit for Gait Assistance. In Robotics and Automation (ICRA), 2015 IEEE International Conference on, p. Seattle, WA.

Awad, L. N., Palmer, J. A., Pohlig, R. T., Binder-Macleod, S. A. and Reisman, D. S. (2015). Walking speed and step length asymmetry modify the energy cost of walking after stroke. *Neurorehabil. Neural Repair* **29**, 416-423.

Awad, L. N., Reisman, D. S., Pohlig, R. T. and Binder-Macleod, S. A. (2016). Reducing the cost of transport and increasing walking distance after stroke. *Neurorehabil. Neural Repair* **30**, 661-670.

Awad, L. N., Bae, J., O'Donnell, K., De Rossi, S. M. M., Hendron, K., Sloot, L. H., Kudzia, P., Allen, S., Holt, K. G., Ellis, T. D., et al. (2017a). A soft robotic exosuit improves walking in patients after stroke. *Sci. Transl. Med.* **9**, eaai9084.

Awad, L. N., Bae, J., Kudzia, P., Long, A., Hendron, K. K., Holt, K. G., O'Donnell, K., Ellis, T. D. Walsh, C. J. (2017b). Reducing circumduction and hip hiking during hemiparetic walking through targeted assistance of the paretic limb using a soft robotic exosuit. *Am. J. Phys. Med. Rehabil.* **96**, 157-164.

Bae, J., Maria De Rossi, S. M., O'Donnell, K., Hendron, K. L., Awad, L. N., Teles Dos Santos, T. R., De Araujo, V. L., Ding, Y., Holt, K. G., Ellis, T. D. et al. (2015). A soft exosuit for patients with stroke: Feasibility study with a mobile off-board actuation unit. Rehabil. Robot. (ICORR), 2015 IEEE Int. Conf. 131-138.

Bonnet, X., Villa, C., Fodé, P., Lavaste, F. and Pillet, H. (2014). Mechanical work performed by individual limbs of transfemoral amputees during step-to-step transitions: effect of walking velocity. *Proc. Inst. Mech. Eng. H.* **228**, 60-66.

Brockway, J. M. (1987). Derivation of formulae used to calculate energy expenditure in man. *Hum. Nutr. Clin. Nutr.* **41**, 463-471.

Chen, G., Patten, C., Kothari, D. H. and Zajac, F. E. (2005). Gait differences between individuals with post-stroke hemiparesis and non-disabled controls at matched speeds. *Gait Posture* **22**, 51-56.

Collins, S. H., Wiggin, M. B. and Sawicki, G. S. (2015). Reducing the energy cost of human walking using an unpowered exoskeleton. *Nature* **522**, 212-215.

Díaz, I., Gil, J. J. and Sánchez, E. (2011). Lower-limb robotic rehabilitation: literature review and challenges. *J. Robot.* **2011**, 1-11.

Ding, Y., Galiana, I., Asbeck, A., Quinlivan, B., De Rossi, S. M. M. and Walsh, C. (2014). Multi-joint actuation platform for lower extremity soft exosuits. In Robotics and Automation (ICRA), 2014 IEEE International Conference on, pp. 1327-1334.

Doets, H. C., Vergouw, D., Veeger, H. E. J. D. and Houdijk, H. (2009). Metabolic cost and mechanical work for the step-to-step transition in walking after successful total ankle arthroplasty. *Hum. Mov. Sci.* **28**, 786-797.

Donelan, J. M., Kram, R. and Kuo, A. D. (2002). Mechanical work for step-to-step transitions is a major determinant of the metabolic cost of human walking. *J. Exp. Biol.* **205**, 3717-3727.

Duclos, C., Nadeau, S., Bourgeois, N., Bouyer, L. and Richards, C. L. (2014). Effects of walking with loads above the ankle on gait parameters of persons with hemiparesis after stroke. *Clin. Biomech.* **29**, 265-271.

Ellis, R. G., Howard, K. C. and Kram, R. (2013). The metabolic and mechanical costs of step time asymmetry in walking. *Proc. Biol. Sci.* **280**, 20122784.

Farris, D. J., Hampton, A., Lewek, M. D. and Sawicki, G. S. (2015). Revisiting the mechanics and energetics of walking in individuals with chronic hemiparesis following stroke: from individual limbs to lower limb joints. *J. Neuroeng. Rehabil.* **12**, 24.

Feng, J., Pierce, R., Do, K. P. and Aiona, M. (2014). Motion of the center of mass in children with spastic hemiplegia: Balance, energy transfer, and work performed by the affected leg vs. the unaffected leg. *Gait Posture* **39**, 570-576.

Finley, J. M. and Bastian, A. J. (2017). Associations between foot placement asymmetries and metabolic cost of transport in hemiparetic gait. *Neurorehabil. Neural Repair* **31**, 168-177.

Forrester, L. W., Roy, A., Hafer-Macko, C., Krebs, H. I. and Macko, R. F. (2016). Task-specific ankle robotics gait training after stroke: a randomized pilot study. *J. Neuroeng. Rehabil.* **13**, 51.

Geyer, H., Seyfarth, A. and Blickhan, R. (2006). Compliant leg behaviour explains basic dynamics of walking and running. *Proc. Biol. Sci.* **273**, 2861-2867.

Gresham, G. E., Fitzpatrick, T. E., Wolf, P. A., McNamara, P. M., Kannel, W. B. and Dawber, T. R. (1975). Residual disability in survivors of stroke–the Framingham study. *N. Engl. J. Med.* **293**, 954-956.

Houdijk, H., Pollmann, E., Groenewold, M., Wiggerts, H. and Polomski, W. (2009). The energy cost for the step-to-step transition in amputee walking. *Gait Posture* **30**, 35-40.

Hsiao, H., Awad, L. N., Palmer, J. A., Higginson, J. S. and Binder-Macleod, S. A. (2016). Contribution of paretic and non-paretic limb peak propulsive forces to changes in walking speed in individuals poststroke. *Neurorehabil. Neural Repair* **30**, 743-752.

Kottink, A. I. R., Oostendorp, L. J. M., Buurke, J. H., Nene, A. V., Hermens, H. J. and IJzerman, M. J. (2004). The orthotic effect of functional electrical stimulation on the improvement of walking in stroke patients with a dropped foot: a systematic review. *Artif. Organs* **28**, 577-586.

Kuo, A. D., Donelan, J. M. and Ruina, A. (2005). Energetic consequences of walking like an inverted pendulum: step-to-step transitions. *Exerc. Sport Sci. Rev.* **33**, 88-97.

Lamontagne, A., Stephenson, J. L. and Fung, J. (2007). Physiological evaluation of gait disturbances post stroke. *Clin. Neurophysiol.* **118**, 717-729.

Lin, P.-Y., Yang, Y.-R., Cheng, S.-J. and Wang, R.-Y. (2006). The relation between ankle impairments and gait velocity and symmetry in people with stroke. *Arch. Phys. Med. Rehabil.* **87**, 562-568.

Lynch, C. L. and Popovic, M. R. (2008). Functional electrical stimulation. *IEEE Control Syst. Mag.* **28**, 40-50.

Mahon, C. E., Farris, D. J., Sawicki, G. S. and Lewek, M. D. (2015). Individual limb mechanical analysis of gait following stroke. *J. Biomech.* **48**, 984-989.

Malcolm, P., Derave, W., Galle, S., De Clercq, D. and Daugherty, S. (2013). A simple exoskeleton that assists plantarflexion can reduce the metabolic cost of human walking. *PLoS ONE* **8**, e56137.

Mooney, L. M., Rouse, E. J., Herr, H. M., Patterson, M., Roberts, W., Lau, W., Prigg, S., Yagn, N., Kazerooni, H., Steger, R. et al. (2014). Autonomous exoskeleton reduces metabolic cost of human walking during load carriage. *J. Neuroeng. Rehabil.* **11**, 80.

Mozaffarian, D., Benjamin, E. J., Go, A. S., Arnett, D. K., Blaha, M. J., Cushman, M., de Ferranti, S., Despres, J.-P., Fullerton, H. J., Howard, V. J. et al. (2015). Heart disease and stroke statistics – 2015 update: a report from the American Heart Association. *Circulation* 131, e29-322.

Nadeau, S. (2014). Understanding spatial and temporal gait asymmetries in individuals post stroke. *Int. J. Phys. Med. Rehabil.* **2**, 201.

Olney, S. and Richards, C. (1996). Hemiparetic gait following stroke. Part I: characteristics. *Gait Posture* **4**, 136-148.

Olney, S. J., Griffin, M. P., Monga, T. N. and McBride, I. D. (1991). Work and power in gait of stroke patients. *Arch. Phys. Med. Rehabil.* **72**, 309-314.

Panizzolo, F. A., Galiana, I., Asbeck, A. T., Siviy, C., Schmidt, K., Holt, K. G. and Walsh, C. J. (2016). A biologically-inspired multi-joint soft exosuit that can reduce the energy cost of loaded walking. *J. Neuroeng. Rehabil.* **13**, 43.

Patterson, K. K., Parafianowicz, I., Danells, C. J., Closson, V., Verrier, M. C., Staines, W. R., Black, S. E. and McIlroy, W. E. (2008). Gait asymmetry in community-ambulating stroke survivors. *Arch. Phys. Med. Rehabil.* **89**, 304-310.

Patterson, K. K., Gage, W. H., Brooks, D., Black, S. E. and McIlroy, W. E. (2010). Changes in gait symmetry and velocity after stroke: a cross-sectional study from weeks to years after stroke. *Neurorehabil. Neural Repair* **24**, 783-790.

Perry, J., Garrett, M., Gronley, J. K. and Mulroy, S. J. (1995). Classification of walking handicap in the stroke population. *Stroke* **26**, 982-989.

Peterson, C. L., Hall, A. L., Kautz, S. A., Neptune, R. R., Topp, E. L. and Rosen, J. M. (2010). Pre-swing deficits in forward propulsion, swing initiation and power generation by individual muscles during hemiparetic walking. *J. Biomech.* **43**, 2348-2355.

Quinlivan, B. T., Lee, S., Malcolm, P., Rossi, D. M., Grimmer, M., Siviy, C., Karavas, N., Wagner, D., Asbeck, A., Galiana, I., et al. (2017). Assistance magnitude versus metabolic cost reductions for a tethered multiarticular soft exosuit. *Science Robotics* **2**, eaah4416.

Shorter, K. A., Kogler, G. F., Loth, E., Durfee, W. K. and Hsiao-wecksler, E. T. (2011). A portable powered ankle-foot orthosis for rehabilitation. *J. Rehabil. Res. Dev.* **48**, 459-472.

Shorter, K. A., Wu, A. and Kuo, A. D. (2017). The high cost of swing leg circumduction during human walking. *Gait Posture*.

Soo, C. H. and Donelan, J. M. (2012). Coordination of push-off and collision determine the mechanical work of step-to-step transitions when isolated from human walking. *Gait Posture* **35**, 292-297.

Stoquart, G., Detrembleur, C. and Lejeune, T. M. (2012). The reasons why stroke patients expend so much energy to walk slowly. *Gait Posture* **36**, 409-413.

Takahashi, K. Z., Kepple, T. M. and Stanhope, S. J. (2012). A unified deformable (UD) segment model for quantifying total power of anatomical and prosthetic below-knee structures during stance in gait. *J. Biomech.* **45**, 2662-2667.

Takahashi, K. Z., Lewek, M. D. and Sawicki, G. S. (2015). A neuromechanics-based powered ankle exoskeleton to assist walking post-stroke: a feasibility study. *J. Neuroeng. Rehabil.* **12**, 23.

Turns, L. J., Neptune, R. R., Kautz, S. A., Duysens, J., McAllister, D. and Beaupre, G. S. (2007). Relationships between muscle activity and anteroposterior ground reaction forces in hemiparetic walking. *Arch. Phys. Med. Rehabil.* **88**, 1127-1135.

van Swigchem, R., Roerdink, M., Weerdesteyn, V., Geurts, A. C. and Daffertshofer, A. (2014). The capacity to restore steady gait after a step modification is reduced in people with poststroke foot drop using an ankle-foot orthosis. *Phys. Ther.* **94**, 654-663.

Vistamehr, A., Kautz, S. A. and Neptune, R. R. (2014). The influence of solid ankle-foot-orthoses on forward propulsion and dynamic balance in healthy adults during walking. *Clin. Biomech.* **29**, 583-589.

Weerdesteyn, V., de Niet, M., van Duijnhoven, H. J. R. and Geurts, A. C. H. (2008). Falls in individuals with stroke. *J. Rehabil. Res. Dev.* **45**, 1195-1213.

Winter, D. A. (2009). *Biomechanics and Motor Control of Human Movement*. Hoboken, NJ: Wiley.

Zelik, K. E. and Adamczyk, P. G. (2016). A unified perspective on ankle push-off in human walking. *J. Exp. Biol.* **219**, 3676-3683.

Zelik, K. E. and Kuo, A. D. (2010). Human walking isn't all hard work: evidence of soft tissue contributions to energy dissipation and return. *J. Exp. Biol.* **213**, 4257-4264.

Zelik, K. E., Takahashi, K. Z. and Sawicki, G. S. (2015). Six degree-of-freedom analysis of hip, knee, ankle and foot provides updated understanding of biomechanical work during human walking. *J. Exp. Biol.* **218**, 876-886.